Dynamic Performance of Induction Motors driven by an Alternative Method of Vector Control

José Wilson Lima Nerys and Asley Stecca Steindorff

Universidade Federal de Goiás
Escola de Engenharia Elétrica
Praça Universitária, s/n, Setor Universitário
74605-220 - Goiânia - GO - Brazil
jwilson@eee.ufg.br

***Abstract* – The paper presents some simulated and experimental results showing the dynamic performance of an induction motor driven by an alternative method of vector control. It includes the dynamic response to change in speed and to change in load under both tuned and detuned operation. Two sets of reference speeds (a square and a sine wave) are used for no load operation and a load system is used to apply load torque to the induction motor at any speed. The simulated results demonstrate the validity of the system model, which was developed in the Matlab/ Simulink® environment, and the experimental results show the rapid dynamic response of the implemented vector control method, as expected from a well adjusted vector control scheme.**

I. INTRODUCTION

The difference between the so-called alternative method of vector control for induction motor [1, 2 and 3] and the standard method [4, 5] is that the former does not make use of the absolute position of any flux-linkage (rotor, stator nor air-gap flux-linkage). Instead, it makes use of the relative position ξ between the absolute position of the rotor flux- linkage vector $\vec{\psi}_r$ and the stator current vector $\vec{i}_s$, as shown in Fig. 1.

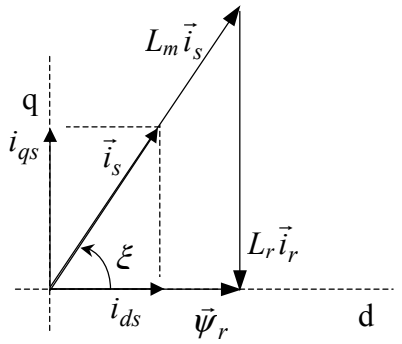

Fig. 1: Rotor flux-linkage and its components

The flux and torque components of the stator current vector, respectively i_{ds} and i_{qs}, are used together with the rotor time constant τ_r to process the magnitude I_s (1), the phase, or relative position, ξ (2) and the slip frequency ω_{sl} (3) of the stator current vector.

$$I_s = \sqrt{i_{ds}^2 + i_{qs}^2} \tag{1}$$

$$\xi = arc\tan\left(\frac{i_{qs}}{i_{ds}}\right) \tag{2}$$

$$\omega_{sl} = \frac{1}{\tau_r}\frac{i_{qs}}{i_{ds}} \tag{3}$$

The slip frequency added to the rotor speed ω_r, results in the synchronous speed, or stator frequency ω_s, which is used together with the magnitude and phase of the stator current vector to generate the three instantaneous stator reference currents (4) from digitally stored sine waves [1].

$$\begin{aligned} i_a^* &= I_s \cos(\theta_s + \xi) \\ i_b^* &= I_s \cos(\theta_s + \xi - 2\pi/3) \\ i_c^* &= I_s \cos(\theta_s + \xi + 2\pi/3) \end{aligned} \tag{4}$$

where $\theta_s = \int \omega_s dt$

The generation process of the three instantaneous stator reference currents is better understood with the aid of Fig.2. This EPROM unit was part of the implemented vector control scheme.

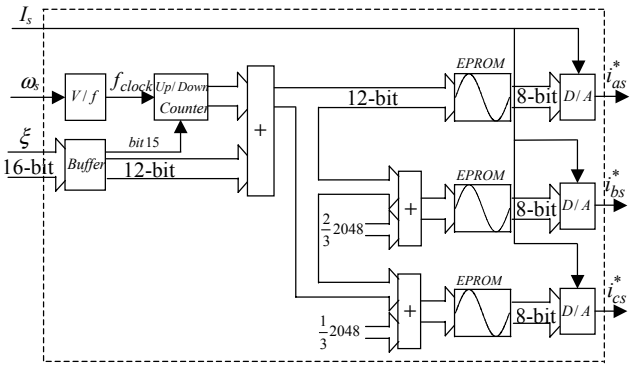

Fig. 2: Instantaneous stator current generation

The stator current magnitude I_s, obtained from (1), is used as a multiplier at the output of the digital to analogue converter. The stator frequency ω_s is used to provide the frequency of reading (EPROM clock frequency) and the relative position ξ provides the necessary jump in the reading address of the EPROMs. At steady state, these three variables I_s, ξ and ω_s are constant values, which results in three instantaneous reference currents with constant magnitude and frequency. When any change is called for, through the torque component of the stator current, the three referred variables change together, so that the magnitude, the frequency and the phase of the stator current are quickly adjusted to the new operating condition. It should be stressed that the phase change is accomplished by changing the address of the EPROM reading, without any need of the absolute position of the rotor flux.

Back to Fig. 1, it also shows the triangle of the rotor flux-linkage defined by expression (5), where the components $L_m\vec{i}_s$ and $L_r\vec{i}_r$ are, respectively, the vectors of the mutual flux and rotor self-flux (L_m is the magnetising inductance and L_r is the rotor self-inductance).

$$\vec{\psi}_r = L_m\vec{i}_s + L_r\vec{i}_r \tag{5}$$

At steady state these three vectors always form a right-angled triangle, with the mutual flux as hypotenuse. The motor torque (6) is proportional to the product of rotor flux-linkage and the torque component of the stator current and, so, it is proportional to the rotor flux triangle area.

$$T_e = k\psi_r i_{qs} \tag{6}$$

The analysis will show that under a correctly tuned vector control algorithm, the magnitude, the position and the speed of the stator current vector change quickly, as a result of a rapid change in the rotor current keeping constant the rotor flux-linkage.

The simulation is performed supposing rated rotor flux-linkage, which means rms value of the flux component of the stator current equal to 2.5 A (i_{ds} = 2.5$\sqrt{2}$ A). The torque component of the stator current is chosen such as to have maximum motor torque equal to 21.7 Nm. The inertia of the complete system is 0.0575 kg.m^2. The experimental results were obtained using a 3-phase, 3.0 kW, 50 Hz, 220-240/380-415 V, 11.2 /6.5 A, 1420 rpm induction motor coupled to a dc machine with field of 110 V / 1.0 A - 0.4 A, and armature of 110 V / 27.3 A, 1500 rpm.

II. DYNAMIC PERFORMANCE

The Simulink® model of the vector controlled induction motor is shown in Fig. 3. The necessary reference speed and load torque are appropriately generated by specific blocks. The reference speed block is able to generate square and sine waves at any frequency and magnitude.

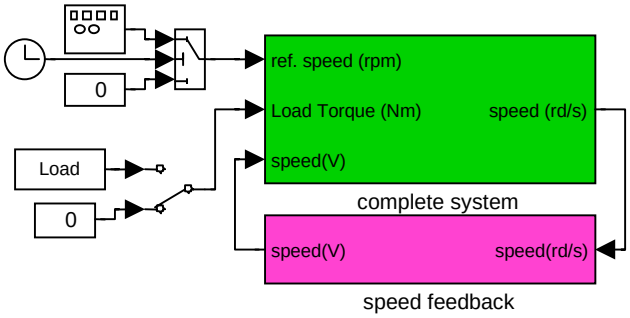

Fig. 3: Complete Simulink® model

The load block allows that load torque be applied and removed at any predefined time. The complete system operates with an inner current loop and an outer speed loop both with PI controllers. The output of the speed controller is the torque component of the stator current, which is used, together with the flux component of the stator current to generate from expressions (1), (2) and (3) the magnitude, the phase and the slip frequency of the instantaneous stator reference currents. Every time the reference speed or the load torque changes, the torque component changes and, consequently, will change the three referred variables. The power amplifier is considered to be ideal and the saturation effects are neglected.

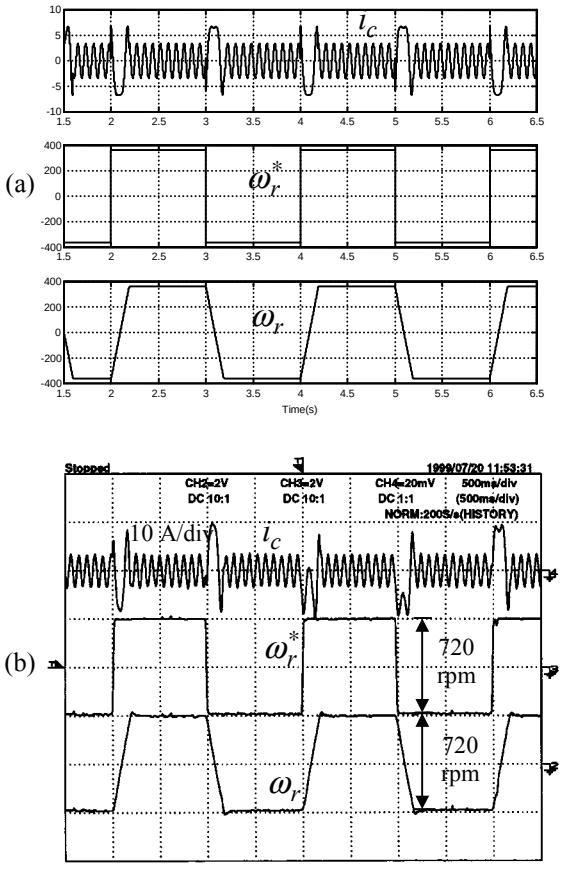

Fig. 4: (a) Simulated and (b) experimental results showing the actual stator current i_c, the square wave reference speed ω_r^* and the actual speed ω_r, with correct rotor time constant (190 ms)

Fig. 4a and Fig. 4b show respectively the simulated and the experimental results for a square wave reference speed, whose frequency is 0.5 Hz and whose magnitude changes between -360 rpm and 360 rpm. The upper trace represents one of the instantaneous stator currents (A), the middle trace represents the reference speed (rpm) and the lower trace represents the actual speed (rpm).

The results show the close similarity between the simulated and the experimental results, which validates the adopted simulation system. The experimental results show that the implemented alternative method of vector control responds quickly and linearly to a speed change demand. The current profile presents a constant magnitude throughout the period of constant reference speed and the speed profile shows a linear variation during the accelerating and the decelerating periods, which indicates a constant motor torque. The increase and decrease times of the actual speed are about 180 ms, as expected from theoretical calculation.

The same approach is used for a sine wave reference speed (Fig. 5) that changes between -360 rpm and 360 rpm at a 0.5 Hz rate. The speed profiles show that the actual speed (lower trace) follows accurately the reference speed (middle trace) in both the simulated and the experimental results. Again the alternative vector control method presented a high dynamic performance.

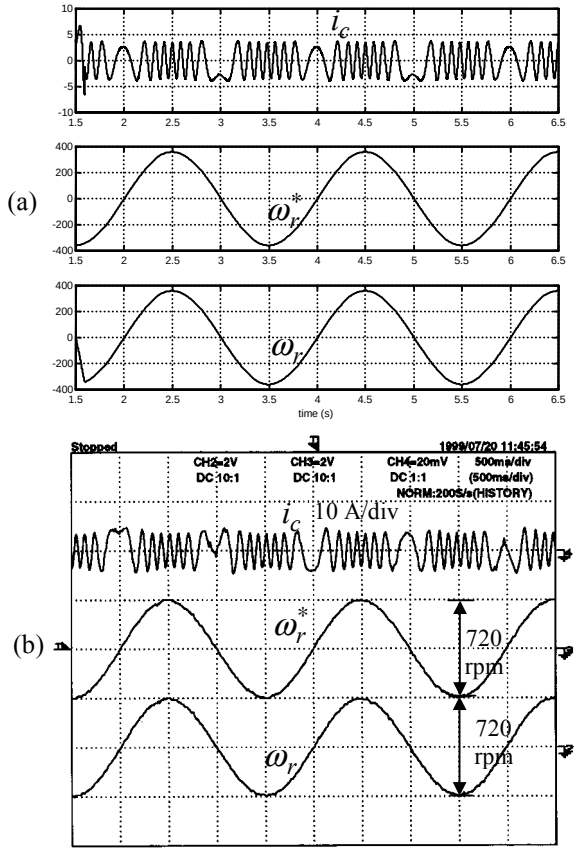

Fig. 5: (a) Simulated and (b) experimental results for a sine wave reference speed ω_r^* with correct rotor time constant

Fig. 6 illustrates the operation under load condition. It shows the simulated and experimental results for the induction motor operating at zero speed (closed loop operation) when a sudden 10 Nm load is applied to the motor.

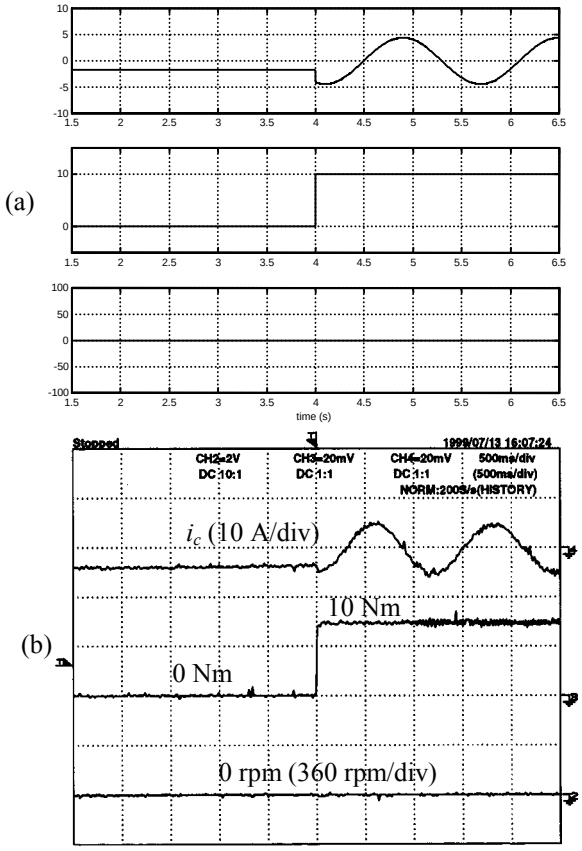

Fig. 6: (a) Simulated and (b) experimental results for change in the load torque at zero speed, with correct rotor time constant

The stator current profile in Fig. 6 shows that initially the motor was at rest and without load (dc magnetising current). When the load is applied the motor reacts with a sudden variation in current such as to produce a motor torque that matches the load torque. The sudden reaction does not cause any undesirable oscillation in the current nor in the speed profile, as expected from a vector control system.

III. DETUNED OPERATION

Before carry out the analyses under detuned condition, some arrangements are necessary in expression (3) of the slip frequency. If an incorrect commanded value for the rotor time constant [$\tau_{r(command)}$] is used in the control algorithm, it will lead to an incorrect command for the slip frequency [$\omega_{sl(command)}$] imposed to the machine. Although this incorrect slip frequency is imposed to the machine, the actual rotor time constant [$\tau_{r(actual)}$] is not changed. Thus, the machine moves toward a new steady state condition in which the ratio between the actual torque component and the actual flux component $(i_{qs}/i_{ds})_{\text{actual}}$ is different from its commanded value and is given by (7).

$$\left(\frac{i_{qs}}{i_{ds}}\right)_{actual} = \omega_{sl(command)}\tau_{r(actual)} \qquad (7)$$

If the command for the rotor time constant is lower than the correct one, the slip frequency imposed to the induction motor will be higher than that one for the tuned condition, as can be evaluated from (3). Results from simulation (Fig. 7) show that the motor moves toward a new operating point with a lower flux level (upper trace) and a higher rotor current (middle trace). As a consequence the mean accelerating torque (lower trace) is lower than that one for tuned condition and, thus, the accelerating rate is smaller.

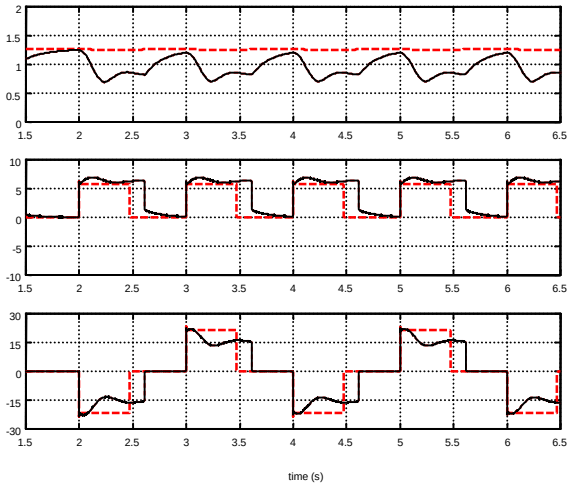

Fig. 7: Rotor flux linkage (upper trace), rotor current magnitude (middle trace) and motor torque (lower trace) for tuned condition (dashed) and for rotor time constant smaller than its correct value (full line)

Although there is a quick torque response at the beginning of each speed variation period shown in Fig. 6, the motor torque moves toward a lower value.

Supposing now that the commanded value of the rotor time constant is higher than its correct value, the imposed slip frequency will be smaller than its correct value. Results from simulation show that in the new steady state of the induction motor the rotor flux level is higher and the rotor current is smaller than their values under tuned condition. As a consequence, the resulting motor torque and thus the accelerating rate is higher than that under tuned condition.

It is clear that the use of an incorrect value for the rotor time constant leads to a non-constant value of rotor flux linkage and, as a consequence, to an oscillatory motor torque profile.

Fig. 8 and 9 illustrate both detuned conditions, for higher and for lower value of rotor time constant in the control algorithm. Both, the simulated and the experimental results are presented. The upper trace represents the stator current, the middle trace is the reference speed and the lower trace is the actual speed.

In Fig. 8 the commanded value for the rotor time constant is 60% its correct value (i.e. 114 ms), while in Fig. 9 the commanded value for the rotor time constant is 140% its correct value (i.e. 266 ms).

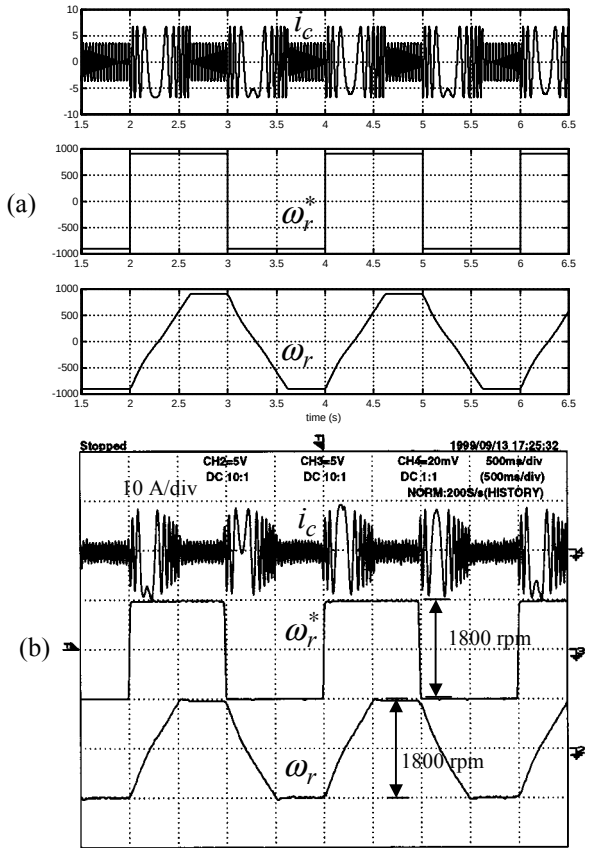

Fig. 8: (a) Simulated and (b) experimental results for commanded value of rotor time constant equal to 60% its correct value

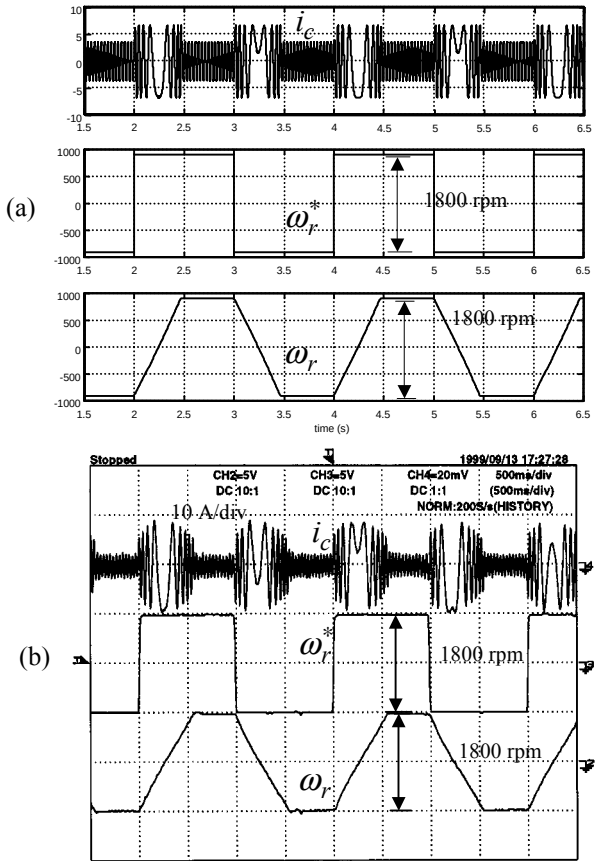

Fig. 9: (a) Simulated and (b) experimental results for commanded value of rotor time constant equal to 140 % its correct value

From the comparison between the simulated and the experimental results in Fig. 8, it can be seen that they are similar in shape but they present some numerical discrepancies. For instance, the simulated accelerating time (about 650 ms) is longer than the experimental value (about 500 ms), which indicates a lower mean value of the accelerating torque for the simulation case. However, there is no undesirable oscillation in the speed or in the current profile.

If the same comparison as before is applied to Fig. 9, it can be concluded that the experimental accelerating torque is lower than the simulated one, resulting in a longer accelerating period.

It should be stressed that, from the analyses carried out before, the higher value for the command of the rotor time constant results in a higher level of rotor flux. However, the practical implementation made use of full flux for the induction motor, through a rated value for the flux component of the stator current. In other words, the rotor flux was already in the saturation region and, therefore, it could not assume a value much higher than the rated one.

IV. ACKNOWLEDGEMENT

The authors are grateful to Fundação de Apoio à Pesquisa – FUNAPE/UFG for the financial support for the presentation of this work.

V. CONCLUSION

The paper presented some simulated and experimental results for an induction motor driven by an alternative vector control method, which does not make use of the rotor flux position information. Both the simulated and the experimental results indicate that the simulation model is suitable for the proposed analyses and that the implemented vector control method leads to a high dynamic performance of the induction motor for speed and for load variation. The experimental results matched the simulated ones for no load operation and they were very close to the experimental results for load and detuned operation. By this stage it has not been possible yet to make a comparison between the alternative method of vector control and the standard one, however this study has been carried out at the Department of the authors.

VI. REFERENCES

[1] J.W.L. Nerys, "An Alternative Implementation of Vector Control for Induction Motors," PhD Thesis, Department of Electronic and Electrical Engineering, The University of Leeds, Leeds, UK, October 1999.

[2] J.W.L. Nerys, A. Hughes and J. Corda, "Alternative Implementation of Vector Control for Induction Motor and its Experimental Evaluation," IEE Proc.-Eletr. Power Appl. Vol. 147, No. 1, January 2000.

[3] A. Hughes, J. □orda and D.A. Andrade, "Vector Control of Cage Induction Motor: A physical Insight," IEE Proc.-Electr. Power Appl., Vol. 143, No. 1, Jan 1996, pp. 59-68.

[4] Blaschke, F.: "The Principle of Field Orientation as Applied to the New Transvector Closed-Loop Control System for Rotating-Field Machines", Siemens Review, 1972, **39**, pp. 217-20.

[5] R. Gabriel, W. Leonard and C. J. Nordby, "Field-Oriented Control of a Standard AC Motor Using Microprocessors," IEEE Trans. on Ind. Appl., vol. IA-16, n. 2, Mar/Apr 1980, pp. 186-92.